Measurement of Silicon Nanoparticles Temperature by Raman Spectroscopy

Alida F. Alykova[1,2*], Maria S. Grigoryeva[1,3], Irina N. Zavestovskaya[1,3], and Victor Yu. Timoshenko[1,3,4]

[1] National Research Nuclear University MEPhI (Moscow Engineering Physics Institute), 31 Kashirskoe shosse, Moscow 115409, Russian Federation

[2] Prokhorov General Physics Institute of RAS, 38 Vavilova str., Moscow 119991, Russian Federation

[3] P. N. Lebedev Physical Institute of the Russian Academy of Sciences, 53 Leninskiy Prospekt, Moscow 199991, Russian Federation

[4] Lomonosov Moscow State University, GSP-1 Leninskie Gory, Moscow 119991, Russian Federation

* e-mail: afalykova@mephi.ru

Abstract. The temperature of silicon nanoparticles under laser photo-induced heating is determined from the ratio of the intensities of the Stokes and anti-Stokes components of the Raman scattering. The obtained results of the dependence of nanoparticles temperature on the laser radiation intensity and the temperature dependence of the Raman line position may be used to determine the optimal regimes of photo-hyperthermia enhanced by silicon nanoparticles for cancer therapy. © 2021 Journal of Biomedical Photonics & Engineering.

1 Introduction

Silicon nanoparticles (Si NPs), including NPs of crystalline and porous silicon, are widely researched for biomedicine applications, in particular, as active elements of biosensors and as part of new drugs for theranostics (simultaneous diagnosis and therapy) of oncological and other socially significant diseases [1–6]. If the size of crystalline NPs is less than 10 nm, they exhibit photoluminescence in the biological transparency window (650–850 nm), which can be used for their visualization in cells and tissues [7–11]. The large Si nanoparticles (more than 10 nm) are in turn capable of providing nonlinear biovisualization mechanisms, such as two-photon luminescence and second harmonic generation, the combination of which makes it possible to effectively track both individual silicon NPs and their aggregation in different parts of the cell, while the resolution of such approach is sufficient to obtain 3D-images [12].

The simultaneous use of the diagnostic functionality of silicon nanoparticles and their therapeutic properties predicts the development of new methods of theranostics, in particular, the theranostics of cancer [13]. One of the fast growing areas of nanobiomedicine is the use of NPs as sensitizers of various therapies. In particular, silicon NPs are used in photohyperthermia techniques as a promising nanomaterial with biocompatible and biodegradable properties [14, 15].

The development of hyperthermia techniques raises the problem of heating temperature determining. There are two main techniques to measure temperature – contact and non-contact. Contact techniques are based on achieving a thermal equilibrium state of the measuring temperature transmitter (temperature sensors) with the studied object during their direct contact. The disadvantages of the contact technique are the distortion of the measured object temperature under introducing a thermometer into it; the temperature of the converter always differs from the actual temperature of the measured object; the temperature measurement range is limited by the properties of the temperature sensors materials. In addition, the problem of temperature measuring the in Si NPs cannot be solved by contact technique. Non-contact temperature measurements are carried out by pyrometers and thermal imagers. Existing non-contact thermal imaging thermometers are based on

measuring the infrared radiation intensity in a non-transparent region for living organisms [15, 16].

In the present work, we selected the Raman scattering spectroscopy method to Si NPs temperature monitor. As is known, the intensity of the Stokes and anti-Stokes lines depends on the temperature as a consequence of the Bose-Einstein statistics for the phonon [17]. Furthermore, the Raman scattering lines frequency changes with temperature due to the anharmonicity of lattice oscillations. In particular, this is realized at sufficiently intense photoexcitation causing the sample to heat up [18, 19]. We studied samples of nanocrystalline silicon (nc-Si) NPs as well as nanocrystalline mesoporous silicon (mPSi) films. The temperature change of the samples was achieved by changing the exciting laser radiation intensity. The experimental data obtained with nc-Si NPs and mPSi films confirmed the theoretical model developed in Ref. [19].

2 Experimental technique

Powders of nc-Si were prepared by plasma-chemical synthesis using a plasmatron and pure (99.9 %) microcrystalline Si [1]. Aqueous suspensions were obtained by adding nc-Si to deionized water to achieve a concentration of 1 g/L. In the experiment, 50 μl drop planted on a metal substrate and dried was used. Silicon NPs have a spherical shape and a wide size distribution in the range from 10 to 150 nm. The size distribution has major maxima at 50–120 nm [4]. An argon laser with λ_{ex} = 514.5 nm and a maximum power of 0.2 W was used as an exciting radiation source. The laser beam was focused on nc-Si sample with 3 μm diameter.

MPSi samples were formed by electrochemical etching substrates of c-Si in an ethanol solution of hydrofluoric acid. The method consists in the formation of mesoporous silicon films with a thickness of 50 to 100 μm, a porosity of 50 to 80%, and a pore size of 2 to 5 nm on the surface of c-Si substrates p-type conductivity with a resistivity of 10 to 50 mOm × cm. The source of exciting radiation for the mPSi heating was a semiconductor laser with a wavelength λ_{ex} = 633 nm and a maximum power of 70 mW.

The Raman spectra of nc-Si samples were taken on the DFS-52 spectrometer in 90-degree scattering geometry. The receiver served working in the photon counting mode a cooled photomultiplier tube PMT–79. The diffraction grating of the spectrometer was 1800 g/mm. The spectral resolution was 0.1 cm^{-1}. The mPSi samples were investigated on a Confotec MR–350 setup equipped with an optical microscope, which allowed us to obtain the micro-Raman spectra with a spatial resolution of the order of 1 μm and a spectral resolution of 1 cm^{-1}.

3 Results and discussion

The Stokes and anti-Stokes Raman spectra of nc-Si samples at different powers are shown in Fig. 1. With the increase of the excitation power level, a shift in the spectra to lower frequencies region is observed, which is

caused by the increase of sample temperature during photoinduced heating [19]. Simultaneously with the increase of the excitation power, a change in the ratio between the Stokes and anti-Stokes scattering components intensities is observed.
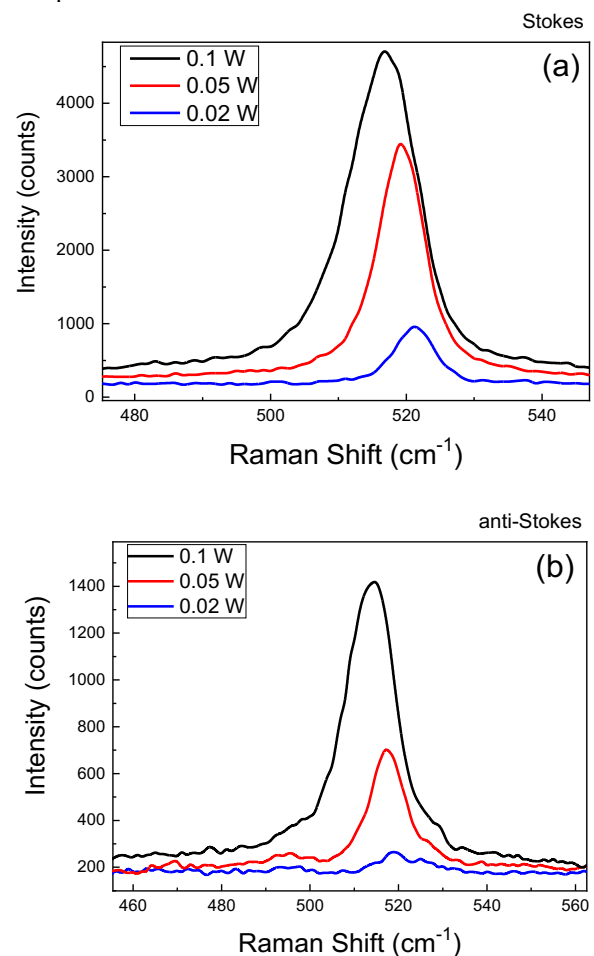

Fig. 1 Raman spectra of nc-Si samples in Stokes (a) and anti-Stokes (b) scattering at λ_{ex} = 514.5 nm.

From the ratio of the Stokes and anti-Stokes components intensities, the NPs temperature can be estimated using the following formula [17, 20]:

$$\frac{I_S}{I_A} \approx exp\left(\frac{\hbar\omega}{kT}\right), \qquad (1)$$

where I_S и I_A are Stokes and anti-Stokes lines intensities, ω is phonon frequency, $k = 1.38 \times 10^{-23}$ J/K, $\hbar = 1.05 \times 10^{-34}$ J×s. Eq. (1) follows from the Bose-Einstein statistics for phonons, neglecting the difference in the absolute values of frequencies and absorption coefficients of the Raman components [17].

Fig. 2 shows the dependence of the I_S / I_A value on the laser radiation intensity, which is almost linear. The decrease of the I_S / I_A value with the increase of the excitation intensity is explained by the photoinduced heating of nc-Si. From Eq. (1), the nc-Si temperature in the excitation region can be estimated by the formula:

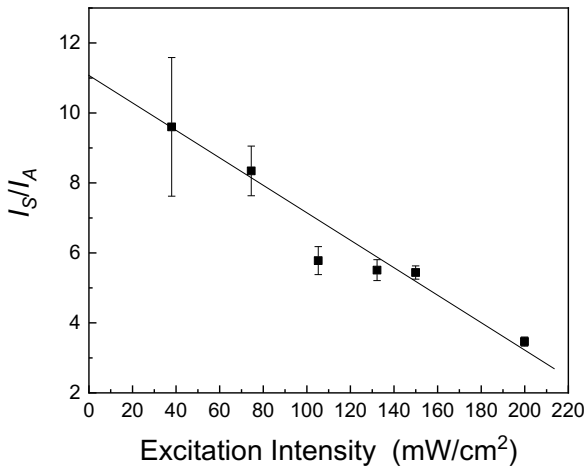$$T = \frac{\hbar\omega}{k \, ln\left(\frac{I_S}{I_A}\right)}. \qquad (2)$$

Fig. 2 Dependence of the ratio of the Stokes and anti-Stokes components intensities on the laser radiation intensity with $\lambda_{ex} = 514.5$ nm.
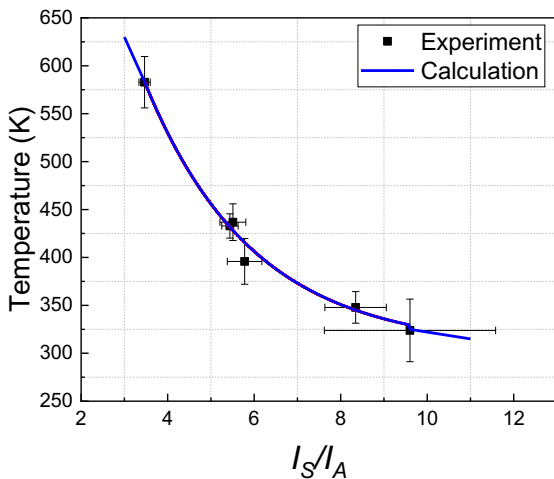

Fig. 3 Temperature dependence of the nc-Si sample on I_S / I_A at $\lambda_{ex} = 514.5$ nm. The dots represent the experimental values.

Fig. 3 shows the experimental values of the nc-Si temperature according to the Raman scattering data and the calculation values by Eq. (2). It can be seen that the experimental error is maximum in the low temperatures region, which corresponds to a very weak photoinduced heating of nc-Si, while the error decreases with increasing temperature. This is occurring due to the increase of the absolute the Raman signals intensities and the decrease of the measurement error of the I_S / I_A ratio. It should be noted that with the increase of the signal accumulation time, the measurement error of the latter value can be reduced to 1%, which will give an accuracy of the temperature determining of the order of 10–15% in the temperature range of 310–320 K.

The dependence of the Raman line shift on the photoinduced heating temperature obtained from the analysis of the spectra in Fig. 1 is shown in Fig. 4. The Raman line temperature shift to the lower frequencies region is in good agreement with the literature data for crystalline and nanocrystalline silicon [18, 19]. The observed linear temperature dependence is convenient to analyze the Si NPs photoinduced heating.
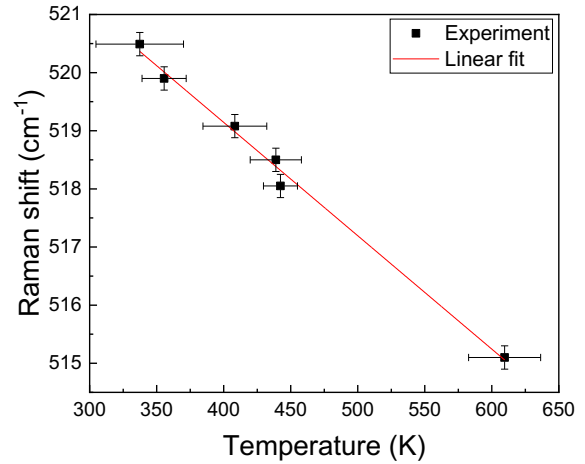

Fig. 4 Raman shift of the nc-Si sample as a function of its temperature at $\lambda_{ex} = 514.5$ nm.

The Stokes Raman spectra of mPSi samples at different powers are shown in Fig. 5. Fig. 6 shows the position of the Raman line maximum, taking into account the data in Fig. 4, as a function of the photoinduced heating temperature. It can be seen that, regardless of the type of nanostructures and the method of their preparation, an almost linear temperature dependence of the Raman peak position is observed. It should be noticed that the absolute positions of the Raman peak frequencies for nc-Si and PSi are 0.5–0.7 cm^{-1} less than those for the c-Si sample taken from the literature, which can be associated with both the accuracy of the Raman frequency determination and with the size effect for phonons in silicon nanocrystals [19].
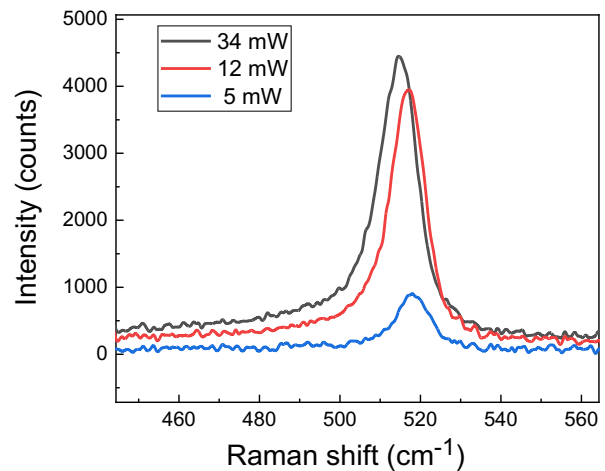

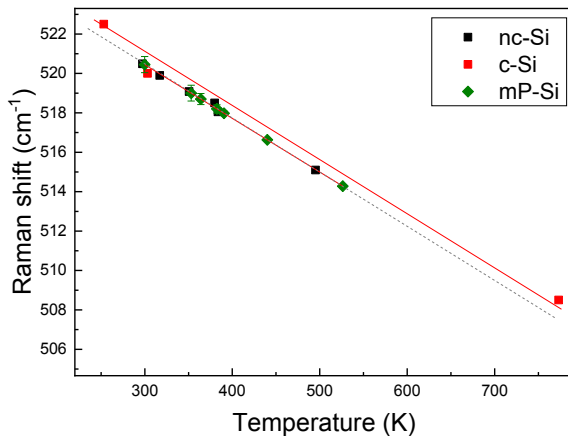Fig. 5 Stokes Raman spectra of mPSi samples at $\lambda_{ex} = 632.5$ nm.

Fig. 6 Raman shifts of the nc-Si sample (black squares) and mPSi (green rhombuses) as a function of temperature, and their approximation (dotted line). The red squares correspond to c-Si [19].

4 Conclusions

The temperature effect of laser radiation on the Raman spectra of nc-Si and mPSi is studied. Measuring the ratio of the Stokes and anti-Stokes components intensities allows us to determine the temperature with a minimum error at temperatures above 350–400 K. It is found that with temperature increase during photoexcitation, the Raman line frequency decreases linearly, which makes it possible to use this dependence to accurately determine the temperature even at low heating.

The results obtained can be used to determine the optimal regimes of photo-hyperthermia upon sensitization with silicon nanocrystals in cancer therapy. The optimal regime of hyperthermia in general, and photo-hyperthermia in particular, is defined by the advisable local temperature, which must be achieved to obtain a therapeutic effect in the selected area, on the one hand, and not leading to irreversible changes in healthy tissues, on the other hand. The temperature shift of the Raman spectrum components observed in silicon nanocrystals allows us to determine the photoinduced heating value with high precision, thus selecting the required radiation power individually in each case.

Disclosures

All authors declare that there is no conflict of interests in this paper.

References

1. A. A. Ischenko, G. V. Fetisov, and L. A. Aslanov, Nanosilicon: Properties, Synthesis,Applications, Methods of Analysis and Control, CRC Press, Boca Raton, USA (2014). ISBN 978-1-4665-9423-4.
2. A. V. Kabashin, V. Yu. Timoshenko, "What theranostic applications could ultra-pure lasersynthesized Si nanoparticles have in cancer?" Nanomedicine 11(17), 2247–2250 (2016).
3. L. A. Osminkina, V. Yu. Timoshenko, "Porous Silicon as a Sensitizer for Biomedical Applications," Mesoporous Biomaterials 3, 39–48 (2016).
4. Yu. V. Kargina, A. M. Perepukhov, A. Yu. Kharin, E. A. Zvereva, A. V. Koshelev, S. V. Zinovyev, A. V. Maximychev, A. F. Alykova, N. V. Sharonova, V. P. Zubov, M. V. Gulyaev, Y. A. Pirogov, A. N. Vasiliev, A. A. Ischenko, and V. Yu. Timoshenko, "Silicon Nanoparticles prepared by plasma-assisted ablative synthesis: physical roperties and potential biomedical applications," Physica Status Solidi A 216(14), 1800897 (2019).
5. V. M. Petriev, V. K. Tischenko, A. A. Mikhailovskaya, A. A. Popov, G. Tselikov, I. Zelepukin, S. M. Deyev, A. D. Kaprin, S. Ivanov, V. Yu. Timoshenko, P. N. Prasad, I. N. Zavestovskaya, and A. V. Kabashin, "Nuclear nanomedicine using Si nanoparticles as safe and effective carriers of 188 Re radionuclide for cancer therapy", Scientific Reports 9(1), 1–10 (2019).
6. S. Kudryashov, A. Nastulyavichus, A. K. Ivanova, N. A. Smirnov, R. A. Khmelnitskiy, A. A. Rudenko, I. N. Saraeva, E. R. Tolordava, A. Yu. Kharin, I. N. Zavestovskaya, Y. M. Romanova, D. A. Zayarny, and A. A. Ionina, "High-throughput laser generation of Si-nanoparticle based surface coatings for antibacterial applications," Applied Surface Science 470, 825–831 (2019).
7. F. Erogbogbo, K. T. Yong, I. Roy, G. X. Xu, P. N. Prasad, and M. T. Swihart, "Biocompatible luminescent silicon quantum dots for imaging of cancer cells," ACS Nano 2(5), 873–878 (2008).
8. M. B. Gongalsky, L. A. Osminkina, A. Pereira, A. A. Manankov, A. A. Fedorenko, A. N. Vasiliev, V. V. Solovyev, A. A. Kudryavtsev, M. Sentis, A. V. Kabashin, and V. Yu. Timoshenko, "Laser-synthesized oxide-passivated bright Si quantum dots for bioimaging," Scientific Reports 6, 24732 (2016).
9. L. Gu, D. J. Hall, Z. Qin, E. Anglin, J. Joo, D. J. Mooney, S. B. Howell, and M. J. Sailor, "In vivo time-gated fluorescence imaging with biodegradable luminescent porous silicon nanoparticles," Nature Communications 4, 2326 (2013).

10. M. O. Morozov, A. V. Kabashin, V. Timoshenko, and I. N. Zavestovskaya, "Photoluminescence properties of silicon nanocrystals grown by nanosecond laser ablation of solid-state targets in an inert gas atmosphere," Bulletin of the Lebedev Physics Institute 44(12), 353–356 (2017).

11. A. F. Alykova, V. G. Yakunin, V. Yu. Timoshenko, and I. N. Zavestovskaya, "Optical methods of silicon nanoparticle diagnostics for applications in biomedicine," Journal of Biomedical Photonics & Engineering 5(2), 020304 (2019).

12. A. Yu. Kharin, V. Lysenko, A. Rogov, Y. V. Ryabchikov, A. Geloen, I. Tishchenko, O. Marty, P. G. Sennikov, R. A. Kornev, I. N. Zavestovskaya, A. V. Kabashin, and V. Yu. Timoshenko, "Bi-Modal Nonlinear Optical Contrast from Si Nanoparticles for Cancer Theranostics," Advanced Optical Materials 7(13), 1801728 (2019).

13. A. V. Kabashin, A. Singh, M. T. Swihart, I. N. Zavestovskaya, and P. N. Prasad, "Laser-Processed Nanosilicon: A Multifunctional nanomaterial for Energy and Healthcare," ACS nano 13(9), 9841–9867 (2019).

14. A. V. Kabashin, K. P. Tamarov, Yu. V. Ryabchikov, L. A. Osminkina, S. V. Zinovyev, J. V. Kargina, M. B. Gongalsky, A. Al-Kattan, V. G. Yakunin, M. Sentis, A. V. Ivanov, V. N. Nikiforov, A. P. Kanavin, I. N. Zavestovskaya, and V. Yu. Timoshenko, "Si nanoparticles as sensitizers for radio frequency-induced cancer hyperthermia," Proceedings of SPIE 9737, 97370A (2016).

15. C. Lee, H. Kim, C. Hong, M. Kim, S. S. Hong, D. H. Lee, and W. I. Lee, "Porous silicon as anagent for cancer thermotherapy based on near-infrared light irradiation," Journal of Materials Chemistry 18(40), 4790–4795 (2008).

16. A. Oleshchenko, A. Yu. Kharin, A. F. Alykova, O. V. Karpukhina, N. V. Karpov, A. A. Popov, V. V. Bezotosnyia, S. M. Klimentov, I. N. Zavestovskaya, A. V. Kabashin, and V. Yu. Timoshenko, "Localized infrared radiation-induced hyperthermia sensitized by laser-ablated silicon nanoparticles for phototherapy applications," Applied Surface Science 516, 145661 (2020).

17. M. Balkanski, R. F. Wallis, and E. Haro, "Anharmonic effects in light scattering due to optical phonons in silicon," Physical Review B 28(4), 1928–1934 (1983).

18. M. J. Konstantinovic, S. Bersier, X. Wang, M. Hayne, P. Lievens, R. E. Silverans, and V. V. Moshchalkov, "Raman scattering in cluster-deposited nanogranular silicon films," Physical Review B 66, 161311(R) (2002).

19. S. S. Périchon, V. Lysenko, B. Remaki, and D. Barbier, "Measurement of porous silicon thermal conductivity by micro-Raman scattering," Journal of Applied Physics 86(8), 4700 (1999).

20. I. H. Campbell, P. M. Fauchet, "The Effects of Microcrystal Size and Shape on the One Phonon Raman Spectra of Crystalline Semiconductors," Solid State Communications 58(10), 739–741 (1986).

21. L. A. Osminkina, K. A. Gonchar, V. S. Marshov, K. V. Bunkov, D. V. Petrov, L. A. Golovan, F. Talkenberg, V. A. Sivakov, and V. Yu. Timoshenko, "Growth, Structure and Optical Properties of Silicon Nanowires Formed by Metal-Assisted Chemical Etching," Nanoscale Research Letters 7(6), 602–606 (2012).